

## Murine Coronavirus Nonstructural Protein p28 Arrests Cell Cycle in G<sub>0</sub>/G<sub>1</sub> Phase

Chun-Jen Chen,<sup>†</sup> Kazuo Sugiyama, Hideyuki Kubo, Cheng Huang, and Shinji Makino\*

*Department of Microbiology and Immunology, The University of Texas Medical Branch at Galveston, Galveston, Texas*

Received 4 March 2004/Accepted 11 May 2004

**Murine coronavirus mouse hepatitis virus (MHV) gene 1 encodes several nonstructural proteins. The functions are unknown for most of these nonstructural proteins, including p28, which is encoded at the 5' end of the MHV genome. Transient expression of cloned p28 in several different cultured cells inhibited cell growth, indicating that p28 expression suppressed cell proliferation. Expressed p28 was exclusively localized in the cytoplasm. Cell cycle analysis by flow cytometry demonstrated that p28 expression induced G<sub>0</sub>/G<sub>1</sub> cell cycle arrest. Characterization of various cellular proteins that are involved in regulating cell cycle progression demonstrated that p28 expression resulted in an accumulation of hypophosphorylated retinoblastoma protein (pRb), tumor suppressor p53, and cyclin-dependent kinase (Cdk) inhibitor p21<sup>Cip1</sup>. Expression of p28 did not alter the amount of p53 transcripts yet increased the amount of p21<sup>Cip1</sup> transcripts, suggesting that p28 expression increased p53 stability and that p21<sup>Cip1</sup> was transcriptionally activated in a p53-dependent manner. Our present data suggest the following model of p28-induced G<sub>0</sub>/G<sub>1</sub> cell cycle arrest. Expressed cytoplasmic p28 induces the stabilization of p53, and accumulated p53 causes transcriptional upregulation of p21<sup>Cip1</sup>. The increased amount of p21<sup>Cip1</sup> suppresses cyclin E/Cdk2 activity, resulting in the inhibition of pRb hyperphosphorylation. Accumulation of hypophosphorylated pRb thus prevents cell cycle progression from G<sub>0</sub>/G<sub>1</sub> to S phase.**

Coronaviruses are enveloped RNA viruses that cause gastrointestinal and upper respiratory tract illnesses in animals and humans (65, 83). These range in severity from very serious neonatal enteritis in domestic animals to the common cold and severe acute respiratory syndrome in humans (24, 35). Mouse hepatitis virus (MHV), a prototypic coronavirus, causes various diseases, including hepatitis, enteritis, and encephalitis in rodents (19, 83). MHV contains a 32 kb-long, positive-sense, single-stranded RNA genome (37, 38, 63) that carries 11 open reading frames (ORFs). Those ORFs are expressed through the production of a genomic-size mRNA and six to eight species of subgenomic mRNAs (36, 39). MHV mRNA 1 encodes the 5'-most gene, the 22-kb-long gene 1, which contains two large overlapping ORFs, ORFs 1a and 1b (8, 38). A ribosomal frameshift that occurs at the 3' end of ORF1a results in the ORF 1a and 1b genes being translated as a large polyprotein (11), which afterward is processed into smaller, mature nonstructural proteins (a total of ~16 proteins) by virus-encoded proteinases (9, 10, 23, 46, 47).

Some of the known functions of the mature gene 1 proteins include RNA polymerase, helicase, and proteinases, but the purposes of most of the other gene 1-encoded proteins are unidentified (28, 38). Analyses of MHV-infected cells demonstrated that the N-terminal cleavage product of gene 1, p28, is detected in the cytoplasm (7) and in cytoplasmic membrane fractions containing viral RNA, helicase and nucleocapsid (N) protein, suggesting that p28 is a component of the putative

MHV replication complex (77). However, the exact role of p28 during MHV infection remains unclear.

Many viruses manipulate the host's cell cycle regulation in order to further their own replication (reviewed in reference 61). Small DNA tumor viruses, such as simian virus 40 (21), adenovirus (34), and human papillomavirus (54), encode proteins that promote cells to enter the S phase. In contrast, herpesviruses, a group of large DNA viruses which encode their own DNA polymerases, generally block cell cycle progression in the G<sub>0</sub>/G<sub>1</sub> phase during lytic infection cycles (reviewed in reference 26). Compared to the number of reports of cell cycle arrest caused by DNA viruses, few reports of RNA virus-induced cell cycle arrest exist. Reovirus infection has been known, for a long time, to inhibit cellular DNA synthesis (20, 29), but not until recently was it shown that the viral  $\sigma$ 1s nonstructural protein mediates reovirus-induced inhibition of cell proliferation by arresting host cells in the G<sub>2</sub>/M phase of the cell cycle (68, 69). Human immunodeficiency virus type 1 infection also induces cell cycle arrest in the G<sub>2</sub>/M phase (30); sole expression of the accessory gene product Vpr is sufficient for inducing G<sub>2</sub>/M cell cycle arrest (70, 72). Vpr-mediated cell cycle arrest apparently favors human immunodeficiency virus type 1 replication, because the long terminal repeat is most active and the expression of viral genome is optimal in the G<sub>2</sub> phase of cell cycle (27). Cell cycle perturbations also are seen in cells infected with the paramyxovirus simian virus (41), measles virus (51, 56), and MHV (16).

Cyclins and cyclin-dependent kinases (Cdks) form complexes and play important regulatory roles in controlling cell cycle progression through the G<sub>1</sub>, S, G<sub>2</sub>, and M phases (reviewed in references 58 and 67). G<sub>1</sub> phase progression requires the activity of cyclin D-Cdk4/6 complexes, and cyclin E-Cdk2 activity is necessary for the G<sub>1</sub>-S transition. These G<sub>1</sub> cyclin-

\* Corresponding author. Mailing address: Department of Microbiology and Immunology, The University of Texas Medical Branch at Galveston, Galveston, TX 77555-1019. Phone: (409) 772-2323. Fax: (409) 772-5065. E-mail: shmakino@utmb.edu.

<sup>†</sup> Present address: Department of Pathology, University of Massachusetts Medical School, Worcester, MA 01655.

Cdk complexes regulate the cell cycle through phosphorylation of the retinoblastoma protein (pRb). In the quiescent G<sub>0</sub> phase, pRb is unphosphorylated; it then is sequentially hypophosphorylated by cyclin D-Cdk4/6 complexes in early G<sub>1</sub> phase and hyperphosphorylated by cyclin E-Cdk2 complex in mid- to late G<sub>1</sub> (48). It remains hyperphosphorylated in the S, G<sub>2</sub>, and M phases of cycling cells (22). In its active, hypophosphorylated state, pRb is a transcriptional repressor when bound to the E2F family of transcription factors. Functionally pRb is inactivated when it is hyperphosphorylated in late G<sub>1</sub>, which results in the release of E2F and allows the transcription of genes that are important for DNA synthesis (reviewed in reference 84). Activities of G<sub>1</sub> cyclin-Cdk complexes are regulated by Cdk inhibitors (CKIs), which can be grouped into two families (reviewed in reference 76). The INK4 family proteins bind to Cdk4 and Cdk6, thus blocking cyclin D-Cdk4/6 activities (reviewed in reference 75). CKIs of Cip/Kip family contain p21<sup>Cip1</sup>, p27<sup>Kip1</sup>, and p57<sup>Kip2</sup>, which are potent inhibitors of cyclin E- and A-dependent Cdk2 (reviewed in reference 55). The tumor suppressor p53 exerts its antiproliferative effect by activating p21<sup>Cip1</sup> (25); however, p21<sup>Cip1</sup> also can be activated by p53-independent mechanisms (78).

The present study demonstrated that expression of MHV p28 had a growth-inhibitory function on the cultured cells in which it was expressed. Expression of p28 induced G<sub>0</sub>/G<sub>1</sub> cell cycle arrest, which was mostly likely due to an increase in the hypophosphorylated form of pRb. The cell cycle block occurred together with the accumulation of p53 and p21<sup>Cip1</sup>, suggesting that p53-mediated activation of p21<sup>Cip1</sup> was one mechanism for p28-induced growth arrest. This is the first demonstration that the expression of an RNA viral nonstructural protein can specifically arrest the cell cycle in the G<sub>0</sub>/G<sub>1</sub> phase.

#### MATERIALS AND METHODS

**Viruses and cells.** Plaque-cloned MHV-A59 and MHV-2 were used in this study. Mouse fibroblast 17Cl-1 cells (82) were cultured as previously described (15). Mouse astrocytoma DBT cells (31) were used for propagation of MHV. Human embryonic lung fibroblast LU cells (3) were cultured as previously described (18). The BOSC23 cells (64) were cultured in Dulbecco's modified Eagle's medium containing 10% fetal calf serum in 10-cm-diameter collagen-coated dishes (BioCoat Collagen I Cellware; Becton Dickinson Labware).

**Plasmid constructions.** A reverse transcription-PCR-based method was used to construct pcDNA 3.1 (Invitrogen)-derived plasmids, pV2-p28-FLAG and pA59-p28-FLAG, each of which contained the FLAG epitope tag at the C termini of the MHV-2 p28 and MHV-A59 p28 ORFs, respectively. Similarly, pEGFP-N1 (Clontech)-derived plasmids, pEGFP-A59-p28 and pEGFP-V2-p28, in which the enhanced green fluorescent protein (EGFP) ORF was fused to the C termini of the MHV-A59 p28 and MHV-2 p28 ORFs, respectively, were created by using a PCR-based method. To construct the plasmid for the Tet-Off gene expression system, the p28-FLAG fragment in pA59-p28-FLAG was subcloned into the NheI-EcoRV sites in pTRE2 (BD Biosciences), yielding pTRE2-p28-FLAG. For retrovirus-mediated expression of p28, the p28-EGFP fragment in pEGFP-A59-p28 and the EGFP gene in pEGFP-N1 were cloned separately into the EcoRI-NotI sites of the retrovirus-based expression vector pCX4bssr (2) to yield pCX-p28EGFP and pCX-EGFP, respectively. The plasmid pcDNA3.1/HisB/LacZ was purchased from Invitrogen.

**Transient p28 expression in 17Cl-1 cells.** Cultures of 17Cl-1 cells growing in six-well plates at 40 to 60% confluence were transfected with 1 µg of various plasmids by using Lipofectamine-Plus reagent (Invitrogen). Transfection efficiency was routinely between 70 to 80%.

**Establishment of p28-expressing 17Cl-1 cell lines.** The Tet-Off-inducible gene expression system (BD Biosciences) was used to generate stable 17Cl-1 cells expressing p28 under the control of tetracycline or its derivative doxycycline. Cultures of 17Cl-1 cells at approximately 50% confluence were transfected with

the pTet-Off plasmid and grown in selection medium containing 600 µg of Geneticin (Invitrogen) per ml for 2 weeks. Cell colonies were isolated and screened by transient transfections with pTRE-Luc for clones with low background and high induction of luciferase in response to doxycycline. One such 17Cl-1/tet-off clone was subsequently cotransfected with pTRE2-p28-FLAG and pTK-Hyg and grown for two weeks in the selection medium containing 600 µg of Geneticin (Invitrogen) per ml, 400 µg of hygromycin B (BD Biosciences) per ml, and 1 µg of doxycycline per ml. Double-stable cell colonies were isolated and screened for p28-FLAG expression (17Cl-1/tet-off-p28) after the withdrawal of doxycycline. Cell clones that did not express p28-FLAG (17Cl-1/tet-off-hyg) were also isolated for use as controls. All transfections were performed with Lipofectamine-Plus reagent (Invitrogen).

**Total cell lysate preparation.** At various times after DNA transfection or doxycycline withdrawal, cells were harvested for total lysate preparation. Cell monolayers were washed once with phosphate-buffered saline and lysed with triple-detergent lysis buffer (50 mM Tris-HCl [pH 8.0], 150 mM NaCl, 0.1% sodium dodecyl sulfate [SDS], 1% NP-40, 0.5% sodium deoxycholate, 1 mM EDTA) containing a protease inhibitor cocktail (Sigma). Cell lysates were collected and incubated on ice for 30 min. After centrifugation at 14,000 × g for 10 min at 4°C, the proteins in the supernatants were quantified (DC protein assay; Bio-Rad) and analyzed by using Western blots. To detect pRb, cells were lysed directly in 1× SDS sample buffer (60 mM Tris-HCl [pH 6.8], 2% SDS, 10% glycerol, 5% 2-mercaptoethanol, 0.01% bromophenol blue), boiled for 10 min, and passed through a 23-gauge needle several times to shear DNA.

**Western blot analysis.** Western blot analysis was performed as previously described (15). The following mouse monoclonal antibodies were used: anti-pRb (G3-245; BD PharMingen) and anti-FLAG (M2, Sigma). The following rabbit polyclonal antibodies were used: anti-p21 (C-19), anti-p53 (FL-393) (Santa Cruz Biotechnology), and anti-p27 (no. 2552; Cell Signaling). Actin was detected by using a goat antiactin polyclonal antibody (I-19; Santa Cruz Biotechnology) as the primary antibody. Suitable secondary antibodies included donkey anti-goat immunoglobulin G and goat anti-mouse and anti-rabbit immunoglobulin Gs conjugated to horseradish peroxidase (Santa Cruz Biotechnology).

**Measurement of cell proliferation.** At 24 h after transfection, 17Cl-1 cells were subcultured into 6-cm-diameter dishes and grown for a further 44 h before being tested for trypan blue exclusion to determine the number of live cells.

**Analyses of subcellular localization of p28.** Cultures of 17Cl-1 cells growing in eight-well coverslip chamber slides (Nunc) at 40 to 60% confluence were transfected with 0.2 µg of pEGFP-N1, pEGFP-A59-p28, or pEGFP-V2-p28. At 24 h after transfection, cultures were incubated with the DNA-binding dye Hoechst 33342 (5 µg/ml) for 5 min, and live cells were observed under a Zeiss LSM 510 UV META laser scanning confocal microscope with excitation wavelengths of 458 and 488 nm in the University of Texas Medical Branch Infectious Disease and Toxicology Optical Imaging Core.

**Cell cycle analysis by flow cytometry.** Nuclear DNA content was measured by using propidium iodide staining and fluorescence-activated cell sorter analysis, as previously described (89). Briefly, adherent cells were trypsinized, washed with phosphate-buffered saline, resuspended in a low-salt stain solution (3% polyethylene glycol 8000, 50 µg of propidium iodide per ml, 0.1% Triton X-100, 4 mM sodium citrate, 10 µg of RNase A per ml), and incubated at 37°C for 20 min. An equal volume of high-salt stain solution (3% polyethylene glycol 8000, 50 µg of propidium iodide per ml, 0.1% Triton X-100, 400 mM sodium chloride) was then added to the cell suspension. Propidium iodide-stained nuclei were stored at 4°C overnight before fluorescence-activated cell sorter analysis (FACScan; Becton-Dickinson), and at least 15,000 nuclei were counted for each sample. ModFit LT V2.0 software (Verity Software House) was used for data analysis.

**Preparation of total cellular RNA and Northern (RNA) blotting.** At various times after doxycycline withdrawal, 17Cl-1/tet-off-p28 cells were harvested for total RNA preparation with an RNAqueous kit (Ambion). Ten micrograms of total RNA was denatured and separated on a 0.8% agarose electrophoretic gel containing formaldehyde, and RNAs were transferred onto nylon filters as previously described (50). Northern blot analysis was performed with digoxigenin-labeled random-primed probes (Roche) corresponding to cDNA fragments of mouse p21<sup>Cip1</sup> (nucleotides [nt] 138 to 412), p53 (nt 782 to 1169), and glyceraldehyde-3-phosphate dehydrogenase (GAPDH) (nt 544 to 1043).

**Retrovirus-mediated p28 expression.** BOSC23 cells at 50 to 60% confluence were transiently cotransfected with 10 µg of pCL-Ampho (57) and either 10 µg of pCX-p28EGFP or 10 µg of pCX-EGFP (control), using the FuGENE 6 transfection reagent (Roche). The medium was replaced with fresh medium at 18 h after transfection, and the pseudotype viruses in the supernatant were collected at 48 h after transfection. The supernatants were filtered through 0.45-µm-pore-size filters, and a 1/100 volume of 0.8-mg/ml Polybrene was added to give a final concentration of 8 µg/ml; this was used as the pseudotype inocu-

lum. The medium from 1-day-old cultures of LU cells that had been plated in 6-cm-diameter dishes was aspirated, and the cells were overlaid with 2 ml of pseudotype inoculum for 4 h. The inoculum was then replaced with fresh growth medium, and the infected cells were incubated at 37°C for 96 h.

## RESULTS

**Expression of p28 inhibits cell proliferation.** To explore possible biological functions of p28, we expressed cloned p28 in mammalian cell cultures and looked for any changes that were induced by its expression. We cloned p28 from two MHV strains, MHV-A59 and MHV-2, into a mammalian expression vector, pcDNA 3.1; proteins MHV-A59 p28 and MHV-2 p28 share 94.3% amino acid identity. The FLAG tag was added at the C terminus of MHV-A59 p28 cDNA and to that of MHV-2 p28 cDNA; the former was named pA59-p28-FLAG plasmid, and the latter was named pV2-p28-FLAG plasmid. A pcDNA 3.1-based vector expressing LacZ, pcDNA3.1/HisB/LacZ, was used as a control. The same amounts of these plasmids were independently transfected into MHV-susceptible 17Cl-1 cells that were about 50% confluent. Judging from the LacZ staining of cells that were transfected with pcDNA3.1/HisB/LacZ, 70 to 80% of the cells were expressing the protein product from the transfected gene. Expression of p28 protein by cells transfected with either the pA59-p28-FLAG plasmid or the pV2-p28-FLAG plasmid was clearly shown at 24 h posttransfection in Western blot analysis of cell extracts with anti-FLAG antibody (Fig. 1A). In repeated experiments, FLAG-tagged MHV-A59 p28 appeared as a single band, whereas FLAG-tagged MHV-2 p28 appeared as two closely migrating bands, with a major fast-migrating signal and a minor slowly migrating signal. Also noted was that the major MHV-2 p28 band migrated slightly more slowly than the MHV-A59 p28 band.

During observation of cells at various times posttransfection, we unexpectedly noticed an apparent growth inhibition in the cells expressing p28 protein derived from both MHV-A59 and MHV-2. The apparent inhibition did not occur in the pcDNA3.1/HisB/LacZ-transfected cells. Neither an increase in the number of dead cells nor enhanced apoptosis was seen in the p28-transfected cells (data not shown), demonstrating that the cell growth inhibition phenomenon was not due to cell death. Counting of live cells at 68 h after transfection revealed that the number of cells in the cultures that were transfected with pA59-p28-FLAG or pV2-p28-FLAG plasmids was about 40% of the cell number in the control cells transfected with pcDNA3.1/HisB/LacZ (Fig. 1B). These data demonstrated that expression of MHV p28 in 17Cl-1 cells inhibited cell proliferation. A similar level of cell proliferation inhibition was also observed in p28-expressing NIH 3T3 cells (data not shown).

**Subcellular localization of expressed p28 in transfected cells.** In MHV-infected cells, synthesized MHV p28 localizes in the cytoplasm (7). As a start to understanding the mechanisms of p28-induced cell growth inhibition, we examined subcellular localization of expressed p28. Immunofluorescence analyses of FLAG-tagged p28-expressing cells did not convincingly reveal the subcellular localization of the expressed p28 (data not shown). To circumvent these technical problems, we constructed a p28-EGFP fusion protein to study the subcellular localization of the expressed p28. The mammalian expression plasmid pEGFP-N1, which expresses EGFP, served as a pa-

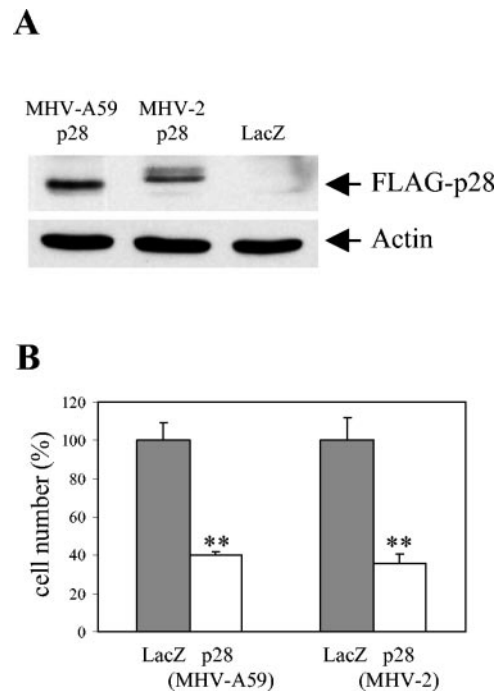


FIG. 1. Transient expression of p28-FLAG inhibited cell proliferation. 17Cl-1 cells cultured in six-well plates were transfected with 1  $\mu$ g of pA59-p28-FLAG, pV2-p28-FLAG, or pcDNA3.1/HisB/LacZ. (A) At 24 h after transfection, cell lysates were prepared and subjected to Western blot analysis with anti-FLAG M2 and antiactin as the primary antibodies. (B) At 68 h after transfection, the numbers of live cells in each sample were determined by using trypan blue exclusion. The results are presented as the mean and standard error of cell numbers for six independent experiments, and the cell numbers in p28-transfected samples were normalized to the cell numbers in LacZ-transfected samples (100%). \*\*,  $P < 0.001$  (Student's *t* test) versus LacZ-transfected samples.

rental plasmid and a negative control. We cloned the p28s of MHV-A59 and MHV-2 into pEGFP-N1, yielding pEGFP-A59-p28 and pEGFP-V2-p28, respectively; these plasmids express a p28-EGFP fusion protein, in which EGFP was fused to the C terminus of p28. Transfection of pEGFP-A59-p28 and pEGFP-V2-p28 into 17Cl-1 cells resulted in inhibition of cell proliferation; at 68 h posttransfection, live cell numbers for the cells transfected with p28-EGFP from either MHV-A59 or MHV-2 were about 40% of those for the cells transfected with pEGFP-N1 (data not shown). These data eliminated the possibility that an addition of the FLAG tag or EGFP sequence to p28 was contributing to cell growth inhibition; it was p28 itself that inhibited cell proliferation. Subcellular localization of expressed EGFP and p28-EGFP in live 17Cl-1 cells was examined under a confocal microscope at 24 h posttransfection. Hoechst staining was used to identify the localization of the nucleus. As shown in Fig. 2A to C, expressed EGFP was present both in the cytoplasm and the nucleus. These results were expected, because EGFP is a small protein (about 30 kDa) and is known to diffuse into the nucleus without active nuclear export and import regulations (59). In marked contrast, both MHV-A59 and MHV-2 p28-EGFP fusion proteins were found exclusively in the cytoplasm (Fig. 2D to I); the



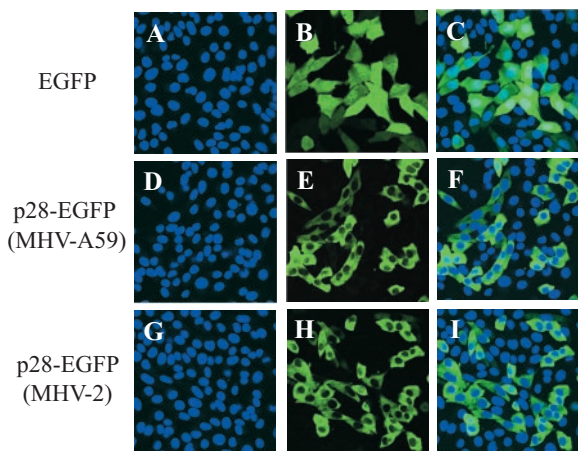


FIG. 2. Subcellular localization of p28-EGFP. 17Cl-1 cells cultured on chambered coverglasses were transfected with pEGFP-N1 (A to C), pEGFP-pA59-p28 (D to F), or pEGFP-pV2-p28 (G to I). At 24 h after transfection, Hoechst 33342 was added to the culture medium, and live cells were observed under a laser confocal microscope with appropriate filters for Hoechst 33342 (blue) (A, D, and G) and EGFP (green) (B, E, and H). Confocal images in the left two columns were superimposed (C, F, and I) to show the cytoplasmic distribution of p28-EGFP.

cytoplasmic localization of p28-EGFP was also observed when the fusion protein was expressed in NIH 3T3 cells (data not shown). These data demonstrated that p28 somehow exerted its inhibitory effect on cell proliferation from its cytoplasmic localization.

**Expression of p28 blocks cell cycle progression in G<sub>0</sub>/G<sub>1</sub>.** To further characterize the p28-induced cell proliferation inhibition, we generated 17Cl-1 cell clones that conditionally expressed FLAG-tagged MHV-A59 p28 by using a Tet-Off system, in which p28 expression is controlled by a tetracycline-regulated promoter. Three 17Cl-1/tet-off-p28 cell clones were isolated and analyzed for FLAG-tagged p28 expression in Western blot analysis with anti-FLAG antibodies (Fig. 3A). When these cells were incubated in the presence of 1 μg of doxycycline per ml, p28 expression was continuously suppressed and cells proliferated normally. Expression of p28 was detectable at 96 h after doxycycline withdrawal from the culture medium, and the expression increased to a higher level at 108 h. Under the microscope, the proliferation of all three cell clones was observed to be inhibited after p28 expression. Most cells were still attached to the culture dishes at 24 h after p28 expression (120 h after doxycycline withdrawal) and appeared morphologically longer than normal 17Cl-1 cells (data not shown). No sign of cell rounding or death was observed in those cells. Three control 17Cl-1/tet-off-hyg cell clones were also isolated, and neither p28 expression nor cell growth inhibition was detected in these cell lines, even at 108 h after doxycycline withdrawal (Fig. 3B).

To determine whether the growth inhibition of p28-expressing cells was due to the arrest of cell cycle progression at a certain phase(s), at 120 h after doxycycline withdrawal, three 17Cl-1/tet-off-p28 cell clones were analyzed for cell cycle profiles by measuring DNA content by propidium iodide staining and flow cytometry (Fig. 4A). The histograms were quantita-

tively analyzed by use of a curve-fitting program to determine the percentage of cells in each of the G<sub>0</sub>/G<sub>1</sub>, S, and G<sub>2</sub>/M phases (Fig. 4B), where G<sub>0</sub>/G<sub>1</sub> phase cells show a 2N DNA content and G<sub>2</sub>/M phase cells show a 4N DNA content. In the presence of doxycycline, all three 17Cl-1/tet-off-p28 cell clones had a normal distribution of cells at G<sub>0</sub>/G<sub>1</sub>, S, and G<sub>2</sub>/M phases, with an average of 50% of the cells in G<sub>0</sub>/G<sub>1</sub>. When cells expressed p28, over 80% of the cells accumulated in the G<sub>0</sub>/G<sub>1</sub> phase, strongly indicating that a G<sub>0</sub>/G<sub>1</sub> cell cycle arrest was induced in p28-expressing cells. In contrast, the cell cycle profiles of all three 17Cl-1/tet-off-hyg cell lines were similar when cells were cultured in the presence or absence of doxycycline, indicating that G<sub>0</sub>/G<sub>1</sub> cell cycle arrest in the 17Cl-1/tet-off-p28 cell clones was rooted in p28 expression and was not a nonspecific effect of doxycycline treatment or treatment withdrawal.

To know whether the p28-induced inhibition of cell cycle progression in G<sub>0</sub>/G<sub>1</sub> phase was due to an overexpression of p28 in 17Cl-1/tet-off-p28 cells, we compared p28 accumulation in MHV-infected cells and p28-expressing 17Cl-1/tet-off-p28 cells. Because anti-p28 antibodies that are suitable for Western blot analysis were not available, a radioimmunoprecipitation method was used to estimate the level of p28 accumulation. We have found that efficient p28 synthesis occurred from 3.5 to

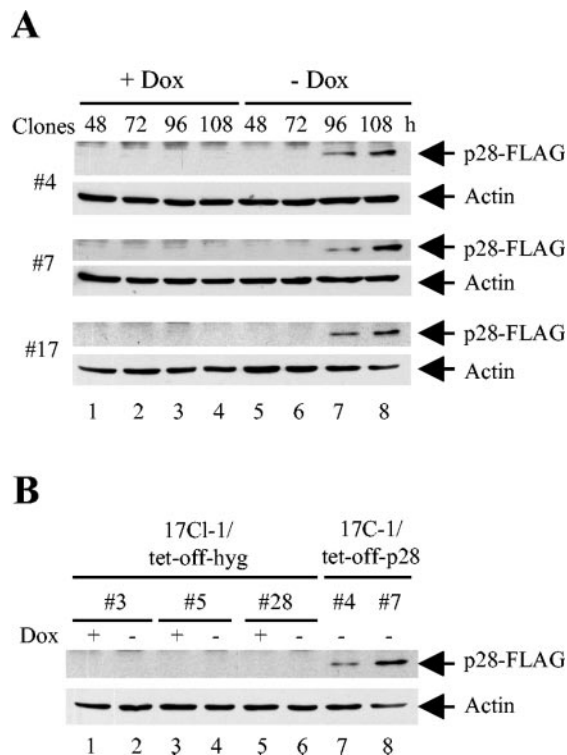


FIG. 3. Tetracycline-regulated p28 expression. (A) 17Cl-1/tet-off-p28 cells were cultured in the presence (+ Dox) or absence (- Dox) of 1 μg of doxycycline per ml. At indicated times after doxycycline withdrawal, cell lysates were collected and subjected to Western blot analysis for FLAG-p28 and actin. (B) Lanes 1 to 6, 17Cl-1/tet-off-hyg cells were cultured in the presence or absence of 1 μg of doxycycline per ml for 108 h, and cell lysates were collected and used in Western blot analysis for FLAG-p28 and actin. Lanes 7 and 8, same samples as in lane 8 of panel A served as positive controls.

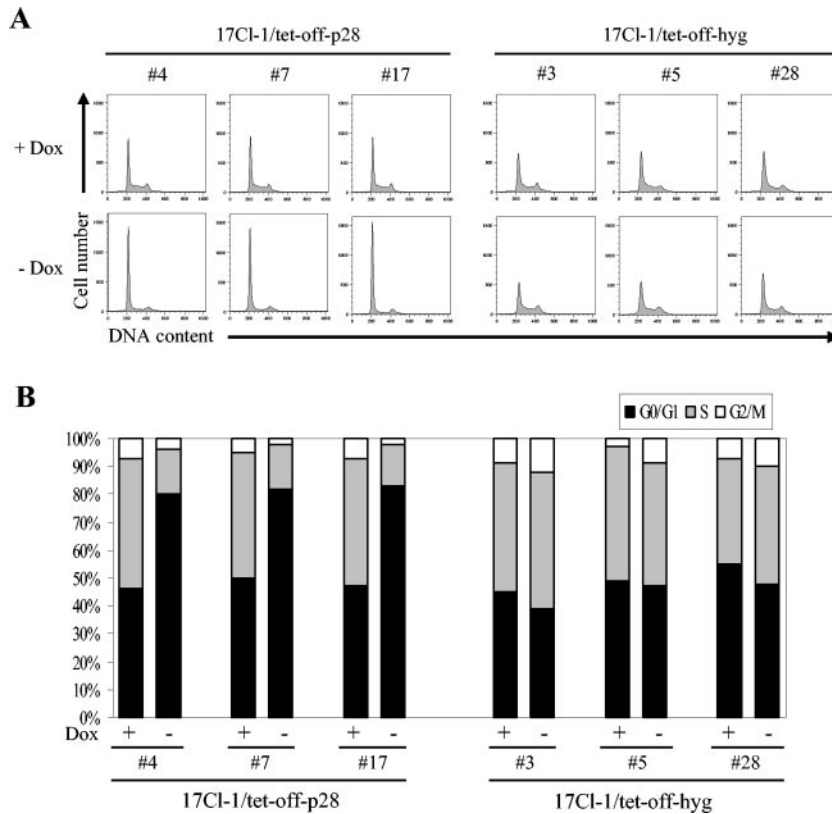


FIG. 4. Cell cycle profiles of p28-expressing cell. (A) 17Cl-1/tet-off-p28 cells and 17Cl-1/tet-off-hyg cells were cultured in the presence (+ Dox) or absence (– Dox) of 1  $\mu$ g of doxycycline per ml. At 120 h after doxycycline withdrawal, cells were collected and subjected to cell cycle analysis as described in Materials and Methods. (B) The percentage of cells in each phase of the cell cycle was computed by using the ModFit LT program. The data represent results from one of three independent experiments; the other two experiments showed similar results.

6.5 h postinfection (p.i.), with the most abundant synthesis occurring at 4.5 h p.i. in MHV-infected cells, and that p28 synthesized early in infection was stable throughout MHV replication (A. Maeda, J. Maeda, and S. Makino, unpublished data); therefore, MHV-A59-infected 17Cl-1 cells were radiolabeled with Tran<sup>35</sup>S-label (ICN) from 3 to 7 h p.i. Similarly, 17Cl-1/tet-off-p28 cells (clone 4) were radiolabeled with Tran<sup>35</sup>S-label from 96 to 101 h or from 108 to 112 h after doxycycline withdrawal. Radioimmunoprecipitation analysis of cell extracts from these cells with anti-p28 antibodies (4) demonstrated that the radiolabeled p28 signals in 17Cl-1/tet-off-p28 cells during both labeling periods were approximately 5% of that in MHV-infected cells (data not shown), indicating that the amount of p28 synthesized and accumulated in the 17Cl-1/tet-off-p28 cells was lower than that in MHV-infected cells. These results indicated that the G<sub>0</sub>/G<sub>1</sub> cell cycle arrest in 17Cl-1/tet-off-p28 cells was not due to overexpression of p28.

**Status of pRb phosphorylation in p28-expressing cells.** Hyperphosphorylation of pRb in late G<sub>1</sub> is necessary for the release of E2F, which then activates genes that are important for DNA synthesis, thereby allowing the cell cycle to progress into the S phase. Accordingly, a possible mechanism of the p28-induced cell cycle progression inhibition in G<sub>0</sub>/G<sub>1</sub> phase may be that p28 expression somehow prevents pRb hyperphosphorylation. We tested this possibility by analyzing the phosphorylation state of pRb in p28-expressing cells by Western

blot analysis with an anti-pRb monoclonal antibody, which detects all forms of pRb. We analyzed total 17Cl-1 cell extracts that were collected at 36 h posttransfection of pcDNA3.1/HisB/LacZ, pA59-p28-FLAG plasmid, or pV2-p28-FLAG plasmid. LacZ-expressing cells had a major slowly migrating pRb band, while cells expressing MHV-2 p28 as well as MHV-A59 p28 had a major fast-migrating pRb band and a minor slowly migrating band (Fig. 5A). The hyperphosphorylated pRb migrates more slowly than the hypo- and unphosphorylated forms of pRb in this experimental condition. Hence, a majority of pRb was the hyperphosphorylated form in LacZ-expressing cells, while the appearance of the major fast-migrating pRb signal in p28-expressing cells indicated accumulation of the hypo- and/or unphosphorylated form. We also examined the phosphorylation state of pRb in 17Cl-1/tet-off-p28 cell clones. As shown in Fig. 5B, when p28 expression was suppressed by doxycycline, pRb remained in a hyperphosphorylated form. After withdrawal of doxycycline to allow p28 expression, an obvious decrease in the hyperphosphorylated pRb and a concomitant accumulation of hypo- and unphosphorylated pRb occurred at 96 and 108 h, during which p28 expression and cell growth arrest were detected (Fig. 3 and 4). Accumulation of hypo- and/or unphosphorylated pRb in p28-expressing cells suggested that p28 expression inhibited pRb hyperphosphorylation, resulting in suppression of E2F activity and progression of the cell cycle to S phase.

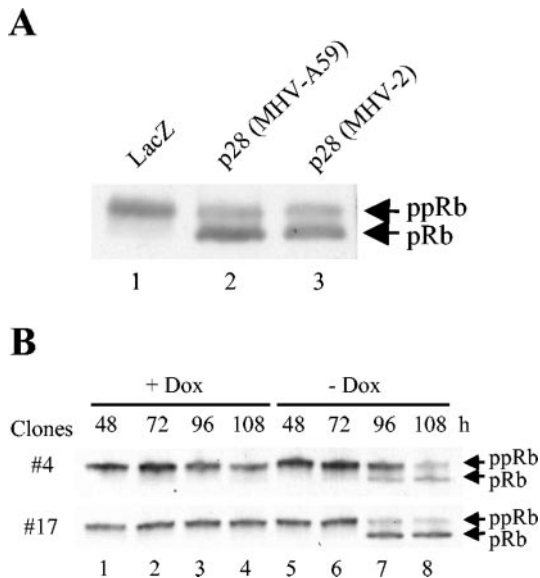


FIG. 5. Phosphorylation status of pRb in p28-expressing cells. (A) 17Cl-1 cells were transfected with 1  $\mu$ g of pA59-p28-FLAG, pV2-p28-FLAG, or pcDNA3.1/HisB/LacZ. At 36 h after transfection, cells were lysed with SDS-polyacrylamide gel electrophoresis sample buffer, and whole-cell lysates were subjected to Western blot analysis for pRb. The slower-migrating band and fast-migrating band are hyperphosphorylated forms of pRb (ppRb) and hypo- and unphosphorylated forms of pRb (pRb), respectively. (B) 17Cl-1/tet-off-p28 cells were cultured in the presence (+ Dox) or absence (- Dox) of 1  $\mu$ g of doxycycline per ml. At the indicated times after doxycycline withdrawal, whole-cell lysates were collected and analyzed as described for panel A.

**Analyses of CKIs and the tumor suppressor p53 in p28-expressing cells.** During cell cycle progression through the G<sub>1</sub> and G<sub>1</sub>-S boundary, pRb is first hypophosphorylated by cyclin D-Cdk4/6 complexes and then hyperphosphorylated by cyclin E-Cdk2 complexes in late G<sub>1</sub>. Accordingly, accumulation of hypo- and/or unphosphorylated pRb in p28-expressing cells indicated inhibition of these G<sub>1</sub> cyclin-Cdk complex functions. CKIs suppress G<sub>1</sub> cyclin-Cdk complex function, and therefore we examined expression levels of two CKIs of the Cip/Kip family in p28-expressing 17Cl-1 cells; these were p21<sup>Cip1</sup> and p27<sup>Kip1</sup>, which can block cyclin E-Cdk2 activity and arrest the cell cycle in G<sub>1</sub>. Cells transfected with pcDNA3.1/HisB/LacZ or pA59-p28-FLAG plasmid were harvested at 36 h after transfection and analyzed for p21<sup>Cip1</sup> and p27<sup>Kip1</sup> expression by Western blot analysis (Fig. 6A). The amounts of p27<sup>Kip1</sup> were similar in LacZ-expressing cells and p28-expressing cells; the slight increase in the amount of p27<sup>Kip1</sup> in p28-expressing cells shown in Fig. 6A was not reproducible. In contrast, p28-expressing cells contained a significantly larger amount of p21<sup>Cip1</sup> than LacZ-expressing cells (Fig. 6A). Furthermore, a significantly large amount of p21<sup>Cip1</sup> was demonstrated at 96 and 108 h after p28 induction in 17Cl-1/tet-off-p28 cells (Fig. 6B). Accumulation of p21<sup>Cip1</sup> protein coincided with that of p28 (Fig. 3) and hypophosphorylated pRb (Fig. 5). We next performed Northern blot analysis of p21<sup>Cip1</sup> to determine whether p21<sup>Cip1</sup> is upregulated at the transcriptional level. As shown in Fig. 6C, 17Cl-1/tet-off-p28 cells demonstrated a very low level of p21<sup>Cip1</sup> mRNA in the absence of p28 expression, while

p21<sup>Cip1</sup> mRNA became detectable at 96 and 108 h after withdrawal of doxycycline, times when p28 expression and p21<sup>Cip1</sup> protein accumulation were evident. We performed these experiments with three different 17Cl-1/tet-off-p28 cell clones and had similar results. These data unquestionably demonstrated that expression of p28 resulted in the activation of p21<sup>Cip1</sup> gene expression.

Because the tumor suppressor protein p53 is known to activate p21<sup>Cip1</sup> transcription (40), we examined whether p53 might have a role in regulating p21<sup>Cip1</sup> expression in p28-expressing cells. Significant p53 accumulation occurred at 96 and 108 h after withdrawal of doxycycline in a 17Cl-1/tet-off-p28 cell clone (Fig. 6B). A similar result was found for two other 17Cl-1/tet-off-p28 cell clones as well (data not shown). Northern blot analysis showed that expression of p28 did not affect the level of p53 mRNA (Fig. 6C), suggesting that p53 accu-

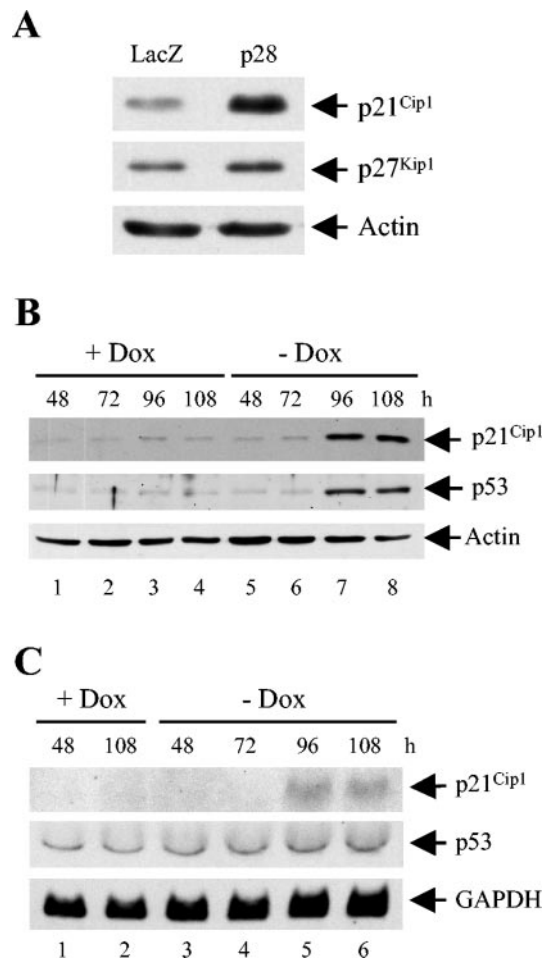


FIG. 6. Accumulation of p21<sup>Cip1</sup> and p53 proteins in p28-expressing cells. (A) 17Cl-1 cells were transfected with 1  $\mu$ g of pA59-p28-FLAG or pcDNA3.1/HisB/LacZ. At 36 h after transfection, cell lysates were collected and subjected to Western blot analysis for p21<sup>Cip1</sup>, p27<sup>Kip1</sup>, and actin. (B and C) 17Cl-1/tet-off-p28 clone 17 cells were cultured in the presence (+ Dox) or absence (- Dox) of 1  $\mu$ g of doxycycline per ml. At the indicated times after doxycycline withdrawal, cell lysates were collected and subjected to Western blot analysis for p21<sup>Cip1</sup>, p53, and actin (B), or total cellular RNA was extracted and equal amounts (10  $\mu$ g) of RNA from each sample were subjected to Northern blot analysis and probed for p21<sup>Cip1</sup>, p53, and GAPDH (C).



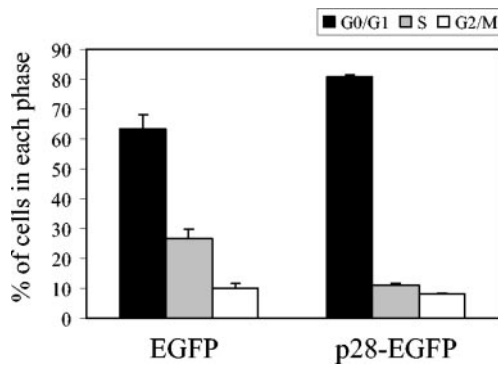


FIG. 7. Cell cycle profiles of p28-expressing LU cells. LU cells were infected with pseudotype retroviruses encoding EGFP or MHV-A59 p28-EGFP fusion protein. At 96 h p.i., cells were collected and subjected to cell cycle analysis by flow cytometry. The percentage of cells in each phase of the cell cycle was computed by using the ModFit LT program. The results are presented as means and standard errors for three independent experiments.

mulation in p28-expressing cells was regulated by a posttranscriptional mechanism(s). These data demonstrated that p28 expression induced p53 accumulation and further suggested that p21<sup>Cip1</sup> was probably activated in a p53-dependent manner.

**Expression of p28 in human embryonic lung fibroblasts results in cell cycle arrest in G<sub>0</sub>/G<sub>1</sub>.** To further establish the association of p53 in p28-mediated cell cycle arrest in G<sub>0</sub>/G<sub>1</sub>, p28 was expressed in LU human embryonic lung fibroblasts (3), which most probably contain wild-type p53, and cell cycle profiles were examined. LU cells responded to a genotoxic chemical insult induced by 1,3-butadiene diepoxide or chlorambucil {4-(4-[bis(2-chloro-ethyl)amino]phenyl)butyric acid} with stabilization of p53, an increase in p53 abundance, and an increase in p21<sup>Cip1</sup> RNA and protein (Z. Chen and T. Albrecht, personal communication). Accordingly, we considered that the use of LU cells was appropriate for the present study. Because LU cells showed poor DNA transfection efficiency (data not shown), we used a retrovirus-based gene delivery method to express p28 in LU cells. Flow cytometric analysis revealed that about 90% of the LU cells were positive for expression of EGFP signal after infection of pseudotype retrovirus-encoding EGFP as well as pseudotype retrovirus-encoding MHV-A59 p28-EGFP fusion protein (data not shown). The numbers of live cells in the cultures that expressed MHV-A59 p28-EGFP fusion protein were approximately 70% of those of control cells expressing EGFP at 96 h p.i. (data not shown), thus demonstrating that cell proliferation was inhibited in human LU cells that expressed p28-EGFP fusion protein. Cell cycle analysis of infected cells at 96 h p.i. showed there was a significant increase in the percentage of cells in the G<sub>0</sub>/G<sub>1</sub> phase, with a reduction in the S phase population of p28-expressing cells, compared with cells expressing EGFP (Fig. 7); the *P* values (Student's *t* test) were less than 0.05 for both G<sub>0</sub>/G<sub>1</sub> and S phases. These studies demonstrated that MHV p28 could induce cell cycle arrest in the G<sub>0</sub>/G<sub>1</sub> phase of human cells, as it could in murine cells.

## DISCUSSION

We demonstrated that expression of p28 in murine 17Cl-1 cells, NIH 3T3 cells, and human LU cells resulted in cell growth retardation. Expressed p28 was detected solely in the cytoplasm. Studies using a tetracycline-regulated p28 expression system in 17Cl-1 cells and pseudotype retrovirus-mediated p28 expression in LU cells revealed that p28 expression led to cell cycle arrest in the G<sub>0</sub>/G<sub>1</sub> phase. To our knowledge, this is the first demonstration that the expression of an RNA viral nonstructural protein can specifically arrest the cell cycle in the G<sub>0</sub>/G<sub>1</sub> phase. Western blot analysis demonstrated that p28 expression induced accumulation of hypophosphorylated pRb, p53, and CKI p21<sup>Cip1</sup> proteins. Northern blot analysis further revealed that p28 expression did not affect the amount of p53 mRNA, yet it increased the amount of p21<sup>Cip1</sup> mRNA. These data suggest a model in which p28 expression induces accumulation of p53, which in turn transcriptionally upregulates p21<sup>Cip1</sup>. The increased amount of p21<sup>Cip1</sup> suppresses cyclin E-Cdk2 complex's function to hyperphosphorylate pRb, resulting in cell cycle arrest in G<sub>0</sub>/G<sub>1</sub> phase (Fig. 8). Wurm et al. showed that expressed transmissible gastroenteritis virus (TGEV) and MHV N proteins localize in both the cytoplasm and the nucleus, particularly in the nucleolus, and that a higher percentage of cells undergo cell division in TGEV N protein-expressing cells; they considered that TGEV N protein causes cell cycle delay or arrest, most likely in the G<sub>2</sub>/M phase (86). If MHV N protein also inhibits cytokinesis, then MHV appears to encode multiple proteins that can affect host cell cycle regulation.

Several herpesvirus proteins that are known to induce cell cycle arrest in G<sub>0</sub>/G<sub>1</sub>, e.g., herpes simplex virus ICP0 and ICP27 (32, 43, 79), Epstein-Barr virus Zta protein (14), and cytomegalovirus IE2 and UL69 proteins (44, 85), are immediate-early gene products that are abundantly synthesized early during lytic infections. As described above, MHV p28 was also

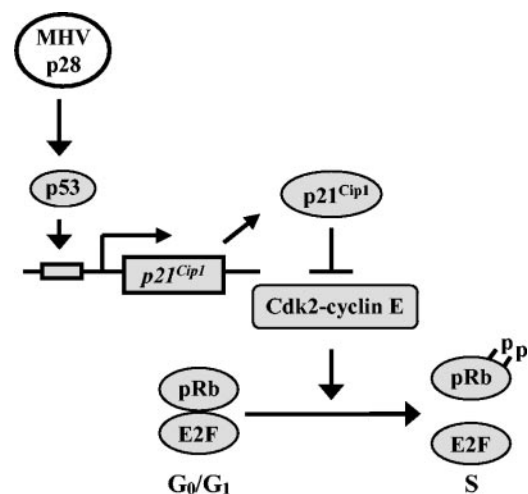


FIG. 8. A model for MHV p28-induced cell cycle arrest in G<sub>0</sub>/G<sub>1</sub> phase. p28 expression induces stabilization and accumulation of p53, which in turn transactivates p21<sup>Cip1</sup>. The upregulated p21<sup>Cip1</sup> suppresses cyclin E-Cdk2 activity, resulting in the inhibition of pRb hyperphosphorylation and the prevention of cell cycle progression from G<sub>0</sub>/G<sub>1</sub> to S phase.

synthesized efficiently early in infection; efficient p28 synthesis occurred from 3.5 to 6.5 h p.i., while the maximum level of viral structural protein synthesis was detected from 6 to 10 h p.i. (A. Maeda, J. Maeda, and S. Makino, unpublished data). Considering the expression time of these antiproliferative viral proteins, certain herpesviruses and MHV might have developed a strategy for suppressing cell cycle progression early in their lytic infection cycles; such modification of the cell cycle regulatory machinery may provide a better cellular environment for efficient viral replication.

The present study suggested that the increased amount of p53 in p28-expressing cells was a factor in inducing p21<sup>Cip1</sup> upregulation. The p53 protein is unstable and has a short half-life, due to its high sensitivity to ubiquitin-mediated proteolysis (62, 71, 73). Stabilization of p53 can be achieved by posttranslational modifications, such as phosphorylation and acetylation, of p53 or by inactivating Mdm2, a cellular inhibitor of p53 (reviewed in references 5 and 6). Some viral proteins are known to affect p53 activities; activation of p53 and p21<sup>Cip1</sup> can be induced by herpes simplex virus ICP0 (32), Epstein-Barr virus Zta (14), cytomegalovirus IE2 (53), and HCV core protein (45). Expressed p28 was detected in the cytoplasm (Fig. 2), while p53 accumulation most probably occurred in the nucleus, implying that cytoplasmic p28 exerts its effect on p53 through activation of a signaling pathway that works across nuclear membranes. Candidate molecules that could be involved in this putative signaling pathway include Mdm2 (33), ATM (13), FRAP/mTOR (88), and p38 (52), all of which affect p53 stability and can shuttle between the cytoplasm and nucleus. Is this putative p28-induced pathway active in MHV-infected cells, and does it have any other biological functions? MHV-2 replication in 17Cl-1 cells and DBT cells arrests the cell cycle in the G<sub>0</sub>/G<sub>1</sub> phase (16). Our study suggested that a reduction in the amounts of G<sub>1</sub> cyclin-Cdk complexes in MHV-infected cells leads to reduced Cdk activities and inefficient hyperphosphorylation of pRb, resulting in inhibition of the cell cycle in the G<sub>0</sub>/G<sub>1</sub> phase. The amounts of CKIs p21<sup>Cip1</sup>, p27<sup>Kip1</sup>, and p16<sup>INK4a</sup> do not change in infected cells, demonstrating that accumulation of p21<sup>Cip1</sup>, which was clearly observed in p28-expressing cells, is masked in MHV-infected cells; MHV-induced general host protein synthesis inhibition may be, at least in part, responsible for preventing accumulation of p21<sup>Cip1</sup>. A putative p28-induced signaling pathway that induces p53 stabilization, however, appeared to be active in MHV-infected cells, because the same specific modification of p53 occurred both in MHV-infected cells and p28-expressing cells (C.-J. Chen, C. Huang, and S. Makino, unpublished data). It is worth noting that ATM and FRAP/mTOR are known to be involved in cap-dependent translation, in addition to their involvement in p53 modification (12, 87). Most coronavirus proteins are translated in a cap-dependent manner, so it will be interesting to examine whether p28 activates a signaling pathway involving ATM and FRAP/mTOR for translational activation of virus-specific proteins.

Binding of cyclin-Cdk complexes to their substrates is mediated through the MRAIL motif in cyclins and a cyclin-binding motif containing the RXL sequence (RXL motif) in the substrates (1, 49, 60, 66, 74). CKIs also bind to cyclins through the CKI's RXL motif (1, 17). Many cyclin-binding proteins have arginine (R) or lysine (K) in the place of X in the RXL

motif, and R of the RXL motif is replaced with K in some cyclin-binding proteins (42). Because MHV p28 has a <sup>109</sup>KRL<sup>111</sup> sequence, which seems to be equivalent to the RXL motif, p28 may bind to cyclins and regulate cyclin-Cdk activities. Besides the RXL motif, the (S/T)PX(K/R) consensus phosphorylation site is present in the substrates of all Cdks (80, 81, 90). MHV-2 p28 contains a <sup>30</sup>SPER<sup>33</sup> sequence in its N-terminal region that is a potential phosphorylation site by Cdks, while MHV-A59 p28 contains an NPER sequence instead of SPER. Western blot analysis resolved MHV-A59 p28 as a single band, while expressed MHV-2 p28 was detectable as two separate bands, a major fast-migrating signal and a minor slowly migrating band (Fig. 1A). It is possible that the slowly migrating band of MHV-2 p28 may represent p28 that was phosphorylated by Cdks. Because MHV-A59 p28 also induces cell cycle arrest, a putative phosphorylation by Cdks is not essential for the antiproliferative function of p28. Nevertheless, besides activating p21<sup>Cip1</sup>, p28 may also bind to the cyclin-Cdk complexes and block cyclin-Cdk activities to induce G<sub>0</sub>/G<sub>1</sub> cell cycle arrest.

#### ACKNOWLEDGMENTS

We thank Zhenping Chen and Thomas Albrecht for LU cells and sharing their unpublished data. We also thank Susan Baker for anti-p28 antiserum and Tsuyoshi Akagi for the pCX4bsr plasmid.

This work was supported by Public Health Service grant AI29984 from the National Institutes of Health.

#### REFERENCES

- Adams, P. D., W. R. Sellers, S. K. Sharma, A. D. Wu, C. M. Nalin, and W. G. Kaelin, Jr. 1996. Identification of a cyclin-cdk2 recognition motif present in substrates and p21-like cyclin-dependent kinase inhibitors. *Mol. Cell. Biol.* **16**:6623–6633.
- Akagi, T., T. Shishido, K. Murata, and H. Hanafusa. 2000. v-Crk activates the phosphoinositide 3-kinase/AKT pathway in transformation. *Proc. Natl. Acad. Sci. USA* **97**:7290–7295.
- Albrecht, T., and T. H. Weller. 1980. Heterogeneous morphologic features of plaques induced by five strains of human cytomegalovirus. *Am. J. Clin. Pathol.* **73**:648–654.
- Baker, S. C., C. K. Shieh, L. H. Soe, M. F. Chang, D. M. Vannier, and M. M. Lai. 1989. Identification of a domain required for autoproteolytic cleavage of murine coronavirus gene A polyprotein. *J. Virol.* **63**:3693–3699.
- Balint, E. E., and K. H. Vousden. 2001. Activation and activities of the p53 tumour suppressor protein. *Br. J. Cancer* **85**:1813–1823.
- Bargonetti, J., and J. J. Manfredi. 2002. Multiple roles of the tumor suppressor p53. *Curr. Opin. Oncol.* **14**:86–91.
- Bi, W., J. D. Pinon, S. Hughes, P. J. Bonilla, K. V. Holmes, S. R. Weiss, and J. L. Leibowitz. 1998. Localization of mouse hepatitis virus open reading frame 1A derived proteins. *J. Neurovirol.* **4**:594–605.
- Bonilla, P. J., A. E. Gorbalenya, and S. R. Weiss. 1994. Mouse hepatitis virus strain A59 RNA polymerase gene ORF 1a: heterogeneity among MHV strains. *Virology* **198**:736–740.
- Bonilla, P. J., S. A. Hughes, J. D. Pinon, and S. R. Weiss. 1995. Characterization of the leader papain-like proteinase of MHV-A59: identification of a new *in vitro* cleavage site. *Virology* **209**:489–497.
- Bonilla, P. J., S. A. Hughes, and S. R. Weiss. 1997. Characterization of a second cleavage site and demonstration of activity *in trans* by the papain-like proteinase of the murine coronavirus mouse hepatitis virus strain A59. *J. Virol.* **71**:900–909.
- Bredenbeek, P. J., C. J. Pachuk, A. F. Noten, J. Charite, W. Luytjes, S. R. Weiss, and W. J. Spaan. 1990. The primary structure and expression of the second open reading frame of the polymerase gene of the coronavirus MHV-A59; a highly conserved polymerase is expressed by an efficient ribosomal frameshifting mechanism. *Nucleic Acids Res.* **18**:1825–1832.
- Brunn, G. J., C. C. Hudson, A. Sekulic, J. M. Williams, H. Hosoi, P. J. Houghton, J. C. Lawrence, Jr., and R. T. Abraham. 1997. Phosphorylation of the translational repressor PHAS-I by the mammalian target of rapamycin. *Science* **277**:99–101.
- Canman, C. E., D. S. Lim, K. A. Cimprich, Y. Taya, K. Tamai, K. Sakaguchi, E. Appella, M. B. Kastan, and J. D. Siliciano. 1998. Activation of the ATM kinase by ionizing radiation and phosphorylation of p53. *Science* **281**:1677–1679.
- Cayrol, C., and E. K. Flemington. 1996. The Epstein-Barr virus bZIP tran-



- scription factor Zta causes G0/G1 cell cycle arrest through induction of cyclin-dependent kinase inhibitors. *EMBO J.* **15**:2748–2759.
15. **Chen, C. J., and S. Makino.** 2002. Murine coronavirus-induced apoptosis in 17Cl-1 cells involves a mitochondria-mediated pathway and its downstream caspase-8 activation and bid cleavage. *Virology* **302**:321–332.
  16. **Chen, C.-J., and S. Makino.** 2004. Murine coronavirus replication induces cell cycle arrest in G<sub>0</sub>/G<sub>1</sub> phase. *J. Virol.* **78**:5658–5669.
  17. **Chen, J., P. Saha, S. Kornbluth, B. D. Dynlacht, and A. Dutta.** 1996. Cyclin-binding motifs are essential for the function of p21CIP1. *Mol. Cell. Biol.* **16**:4673–4682.
  18. **Chen, Z., E. Knutson, A. Kurosky, and T. Albrecht.** 2001. Degradation of p21cip1 in cells productively infected with human cytomegalovirus. *J. Virol.* **75**:3613–3625.
  19. **Compton, S. R., S. W. Barthold, and A. L. Smith.** 1993. The cellular and molecular pathogenesis of coronaviruses. *Lab. Anim. Sci.* **43**:15–28.
  20. **Cox, D. C., and J. E. Shaw.** 1974. Inhibition of the initiation of cellular DNA synthesis after reovirus infection. *J. Virol.* **13**:760–761.
  21. **DeCaprio, J. A., J. W. Ludlow, J. Figue, J. Y. Shew, C. M. Huang, W. H. Lee, E. Marsilio, E. Paucha, and D. M. Livingston.** 1988. SV40 large tumor antigen forms a specific complex with the product of the retinoblastoma susceptibility gene. *Cell* **54**:275–283.
  22. **DeCaprio, J. A., J. W. Ludlow, D. Lynch, Y. Furukawa, J. Griffin, H. Piwnica-Worms, C. M. Huang, and D. M. Livingston.** 1989. The product of the retinoblastoma susceptibility gene has properties of a cell cycle regulatory element. *Cell* **58**:1085–1095.
  23. **Dong, S., and S. C. Baker.** 1994. Determinants of the p28 cleavage site recognized by the first papain-like cysteine proteinase of murine coronavirus. *Virology* **204**:541–549.
  24. **Drosten, C., S. Gunther, W. Preiser, S. van der Werf, H. R. Brodt, S. Becker, H. Rabenau, M. Panning, L. Kolesnikova, R. A. Fouchier, A. Berger, A. M. Burguier, J. Cinatl, M. Eickmann, N. Escriou, K. Grywna, S. Kramme, J. C. Manuguerra, S. Muller, V. Rickerts, M. Sturmer, S. Vieth, H. D. Klenk, A. D. Osterhaus, H. Schmitz, and H. W. Doerr.** 2003. Identification of a novel coronavirus in patients with severe acute respiratory syndrome. *N. Engl. J. Med.* **348**:1967–1976.
  25. **el-Deiry, W. S., T. Tokino, V. E. Velculescu, D. B. Levy, R. Parsons, J. M. Trent, D. Lin, W. E. Mercer, K. W. Kinzler, and B. Vogelstein.** 1993. WAF1, a potential mediator of p53 tumor suppression. *Cell* **75**:817–825.
  26. **Flemington, E. K.** 2001. Herpesvirus lytic replication and the cell cycle: arresting new developments. *J. Virol.* **75**:4475–4481.
  27. **Goh, W. C., M. E. Rogel, C. M. Kinsey, S. F. Michael, P. N. Fultz, M. A. Nowak, B. H. Hahn, and M. Emerman.** 1998. HIV-1 Vpr increases viral expression by manipulation of the cell cycle: a mechanism for selection of Vpr in vivo. *Nat. Med.* **4**:65–71.
  28. **Gorbalenya, A. E., E. V. Koonin, and M. M. Lai.** 1991. Putative papain-related thiol proteases of positive-strand RNA viruses. Identification of rubi- and aphthovirus proteases and delineation of a novel conserved domain associated with proteases of rubi-, alpha- and coronaviruses. *FEBS Lett.* **288**:201–205.
  29. **Hand, R., and I. Tamm.** 1974. Initiation of DNA replication in mammalian cells and its inhibition by reovirus infection. *J. Mol. Biol.* **82**:175–183.
  30. **He, J., S. Choe, R. Walker, P. Di Marzio, D. O. Morgan, and N. R. Landau.** 1995. Human immunodeficiency virus type 1 viral protein R (Vpr) arrests cells in the G<sub>2</sub> phase of the cell cycle by inhibiting p34cdc2 activity. *J. Virol.* **69**:6705–6711.
  31. **Hirano, N., K. Fujiwara, S. Hino, and M. Matsumoto.** 1974. Replication and plaque formation of mouse hepatitis virus (MHV-2) in mouse cell line DBT culture. *Arch. Fesamte Virusforsch.* **44**:298–302.
  32. **Hobbs, W. E., II, and N. A. DeLuca.** 1999. Perturbation of cell cycle progression and cellular gene expression as a function of herpes simplex virus ICP0. *J. Virol.* **73**:8245–8255.
  33. **Honda, R., H. Tanaka, and H. Yasuda.** 1997. Oncoprotein MDM2 is a ubiquitin ligase E3 for tumor suppressor p53. *FEBS Lett.* **420**:25–27.
  34. **Howe, J. A., J. S. Mymryk, C. Egan, P. E. Branton, and S. T. Bayley.** 1990. Retinoblastoma growth suppressor and a 300-kDa protein appear to regulate cellular DNA synthesis. *Proc. Natl. Acad. Sci. USA* **87**:5883–5887.
  35. **Ksiazek, T. G., D. Erdman, C. S. Goldsmith, S. R. Zaki, T. Peret, S. Emery, S. Tong, C. Urbani, J. A. Comer, W. Lim, P. E. Rollin, S. F. Dowell, A. E. Ling, C. D. Humphrey, W. J. Shieh, J. Guarner, C. D. Paddock, P. Rota, B. Fields, J. DeRisi, J. Y. Yang, N. Cox, J. M. Hughes, J. W. LeDuc, W. J. Bellini, and L. J. Anderson.** 2003. A novel coronavirus associated with severe acute respiratory syndrome. *N. Engl. J. Med.* **348**:1953–1966.
  36. **Lai, M. M., P. R. Brayton, R. C. Armen, C. D. Patton, C. Pugh, and S. A. Stohlman.** 1981. Mouse hepatitis virus A59: mRNA structure and genetic localization of the sequence divergence from hepatotropic strain MHV-3. *J. Virol.* **39**:823–834.
  37. **Lai, M. M., and S. A. Stohlman.** 1978. RNA of mouse hepatitis virus. *J. Virol.* **26**:236–242.
  38. **Lee, H. J., C. K. Shieh, A. E. Gorbalenya, E. V. Koonin, N. La Monica, J. Tuler, A. Bagdzhadzhyan, and M. M. Lai.** 1991. The complete sequence (22 kilobases) of murine coronavirus gene 1 encoding the putative proteases and RNA polymerase. *Virology* **180**:567–582.
  39. **Leibowitz, J. L., K. C. Wilhelmsen, and C. W. Bond.** 1981. The virus-specific intracellular RNA species of two murine coronaviruses: MHV-a59 and MHV-JHM. *Virology* **114**:39–51.
  40. **Levine, A. J.** 1997. p53, the cellular gatekeeper for growth and division. *Cell* **88**:323–331.
  41. **Lin, G. Y., and R. A. Lamb.** 2000. The paramyxovirus simian virus 5 V protein slows progression of the cell cycle. *J. Virol.* **74**:9152–9166.
  42. **Lin, X., P. Nelson, and I. H. Gelman.** 2000. SSeCKS, a major protein kinase C substrate with tumor suppressor activity, regulates G<sub>1</sub>→S progression by controlling the expression and cellular compartmentalization of cyclin D. *Mol. Cell. Biol.* **20**:7259–7272.
  43. **Lomonte, P., and R. D. Everett.** 1999. Herpes simplex virus type 1 immediate-early protein Vmw110 inhibits progression of cells through mitosis and from G<sub>1</sub> into S phase of the cell cycle. *J. Virol.* **73**:9456–9467.
  44. **Lu, M., and T. Shenk.** 1999. Human cytomegalovirus UL69 protein induces cells to accumulate in G<sub>1</sub> phase of the cell cycle. *J. Virol.* **73**:676–683.
  45. **Lu, W., S. Y. Lo, M. Chen, K. Wu, Y. K. Fung, and J. H. Ou.** 1999. Activation of p53 tumor suppressor by hepatitis C virus core protein. *Virology* **264**:134–141.
  46. **Lu, X. T., A. C. Sims, and M. R. Denison.** 1998. Mouse hepatitis virus 3C-like protease cleaves a 22-kilodalton protein from the open reading frame 1a polyprotein in virus-infected cells and in vitro. *J. Virol.* **72**:2265–2271.
  47. **Lu, Y., X. Lu, and M. R. Denison.** 1995. Identification and characterization of a serine-like proteinase of the murine coronavirus MHV-A59. *J. Virol.* **69**:3554–3559.
  48. **Lundberg, A. S., and R. A. Weinberg.** 1998. Functional inactivation of the retinoblastoma protein requires sequential modification by at least two distinct cyclin-cdk complexes. *Mol. Cell. Biol.* **18**:753–761.
  49. **Ma, T., N. Zou, B. Y. Lin, L. T. Chow, and J. W. Harper.** 1999. Interaction between cyclin-dependent kinases and human papillomavirus replication-initiation protein E1 is required for efficient viral replication. *Proc. Natl. Acad. Sci. USA* **96**:382–387.
  50. **Makino, S., M. Joo, and J. K. Makino.** 1991. A system for study of coronavirus mRNA synthesis: a regulated, expressed subgenomic defective interfering RNA results from intergenic site insertion. *J. Virol.* **65**:6031–6041.
  51. **McChesney, M. B., A. Altman, and M. B. Oldstone.** 1988. Suppression of T lymphocyte function by measles virus is due to cell cycle arrest in G<sub>1</sub>. *J. Immunol.* **140**:1269–1273.
  52. **Milne, D. M., D. G. Campbell, F. B. Caudwell, and D. W. Meek.** 1994. Phosphorylation of the tumor suppressor protein p53 by mitogen-activated protein kinases. *J. Biol. Chem.* **269**:9253–9260.
  53. **Muganda, P., O. Mendoza, J. Hernandez, and Q. Qian.** 1994. Human cytomegalovirus elevates levels of the cellular protein p53 in infected fibroblasts. *J. Virol.* **68**:8028–8034.
  54. **Munger, K., B. A. Werness, N. Dyson, W. C. Phelps, E. Harlow, and P. M. Howley.** 1989. Complex formation of human papillomavirus E7 proteins with the retinoblastoma tumor suppressor gene product. *EMBO J.* **8**:4099–4105.
  55. **Nakayama, K.** 1998. Cip/Kip cyclin-dependent kinase inhibitors: brakes of the cell cycle engine during development. *Bioessays* **20**:1020–1029.
  56. **Naniche, D., S. I. Reed, and M. B. Oldstone.** 1999. Cell cycle arrest during measles virus infection: a G<sub>0</sub>-like block leads to suppression of retinoblastoma protein expression. *J. Virol.* **73**:1894–1901.
  57. **Naviaux, R. K., E. Costanzi, M. Haas, and I. M. Verma.** 1996. The pCL vector system: rapid production of helper-free, high-titer, recombinant retroviruses. *J. Virol.* **70**:5701–5705.
  58. **Obaya, A. J., and J. M. Sedivy.** 2002. Regulation of cyclin-Cdk activity in mammalian cells. *Cell Mol. Life Sci.* **59**:126–142.
  59. **Ogawa, H., S. Inouye, F. I. Tsuji, K. Yasuda, and K. Umehono.** 1995. Localization, trafficking, and temperature-dependence of the Aequorea green fluorescent protein in cultured vertebrate cells. *Proc. Natl. Acad. Sci. USA* **92**:11899–11903.
  60. **Ohtoshi, A., T. Maeda, H. Higashi, S. Ashizawa, M. Yamada, and M. Hatakeyama.** 2000. beta3-endonexin as a novel inhibitor of cyclin A-associated kinase. *Biochem. Biophys. Res. Commun.* **267**:947–952.
  61. **Op De Beeck, A., and P. Caillet-Fauquet.** 1997. Viruses and the cell cycle. *Prog. Cell Cycle Res.* **3**:1–19.
  62. **Oren, M., W. Maltzman, and A. J. Levine.** 1981. Posttranslational regulation of the 54K cellular tumor antigen in normal and transformed cells. *Mol. Cell. Biol.* **1**:101–110.
  63. **Pachuk, C. J., P. J. Bredenbeek, P. W. Zoltick, W. J. Spaan, and S. R. Weiss.** 1989. Molecular cloning of the gene encoding the putative polymerase of mouse hepatitis coronavirus, strain A59. *Virology* **171**:141–148.
  64. **Pear, W. S., G. P. Nolan, M. L. Scott, and D. Baltimore.** 1993. Production of high-titer helper-free retroviruses by transient transfection. *Proc. Natl. Acad. Sci. USA* **90**:8392–8396.
  65. **Pearlman, S.** 1998. Pathogenesis of coronavirus-induced infections. Review of pathological and immunological aspects. *Adv. Exp. Med. Biol.* **440**:503–513.
  66. **Petersen, B. O., J. Lukas, C. S. Sorensen, J. Bartek, and K. Helin.** 1999. Phosphorylation of mammalian CDC6 by cyclin A/CDK2 regulates its subcellular localization. *EMBO J.* **18**:396–410.
  67. **Pines, J.** 1993. Cyclins and cyclin-dependent kinases: take your partners. *Trends Biochem. Sci.* **18**:195–197.

68. **Poggioli, G. J., T. S. Dermody, and K. L. Tyler.** 2001. Reovirus-induced  $\sigma$ 1s-dependent G<sub>2</sub>/M phase cell cycle arrest is associated with inhibition of p34 (cdc2). *J. Virol.* **75**:7429–7434.
69. **Poggioli, G. J., C. Keefer, J. L. Connolly, T. S. Dermody, and K. L. Tyler.** 2000. Reovirus-induced G<sub>2</sub>/M cell cycle arrest requires  $\sigma$ 1s and occurs in the absence of apoptosis. *J. Virol.* **74**:9562–9570.
70. **Re, F., D. Braaten, E. K. Franke, and J. Luban.** 1995. Human immunodeficiency virus type 1 Vpr arrests the cell cycle in G<sub>2</sub> by inhibiting the activation of p34cdc2-cyclin B. *J. Virol.* **69**:6859–6864.
71. **Reihnsaus, E., M. Kohler, S. Kraiss, M. Oren, and M. Montenarh.** 1990. Regulation of the level of the oncoprotein p53 in non-transformed and transformed cells. *Oncogene* **5**:137–145.
72. **Rogel, M. E., L. I. Wu, and M. Emerman.** 1995. The human immunodeficiency virus type 1 vpr gene prevents cell proliferation during chronic infection. *J. Virol.* **69**:882–888.
73. **Scheffner, M., B. A. Werness, J. M. Huibregtse, A. J. Levine, and P. M. Howley.** 1990. The E6 oncoprotein encoded by human papillomavirus types 16 and 18 promotes the degradation of p53. *Cell* **63**:1129–1136.
74. **Schulman, B. A., D. L. Lindstrom, and E. Harlow.** 1998. Substrate recruitment to cyclin-dependent kinase 2 by a multipurpose docking site on cyclin A. *Proc. Natl. Acad. Sci. USA* **95**:10453–10458.
75. **Shapiro, G. I., C. D. Edwards, and B. J. Rollins.** 2000. The physiology of p16(INK4A)-mediated G1 proliferative arrest. *Cell Biochem. Biophys.* **33**:189–197.
76. **Sherr, C. J., and J. M. Roberts.** 1999. CDK inhibitors: positive and negative regulators of G1-phase progression. *Genes Dev.* **13**:1501–1512.
77. **Sims, A. C., J. Ostermann, and M. R. Denison.** 2000. Mouse hepatitis virus replicase proteins associate with two distinct populations of intracellular membranes. *J. Virol.* **74**:5647–5654.
78. **Somasundaram, K., H. Zhang, Y. X. Zeng, Y. Houvras, Y. Peng, G. S. Wu, J. D. Licht, B. L. Weber, and W. S. El-Deiry.** 1997. Arrest of the cell cycle by the tumour-suppressor BRCA1 requires the CDK-inhibitor p21WAF1/Cip1. *Nature* **389**:187–190.
79. **Song, B., K. C. Yeh, J. Liu, and D. M. Knipe.** 2001. Herpes simplex virus gene products required for viral inhibition of expression of G1-phase functions. *Virology* **290**:320–328.
80. **Songyang, Z., S. Blechner, N. Hoagland, M. F. Hoekstra, H. Piwnica-Worms, and L. C. Cantley.** 1994. Use of an oriented peptide library to determine the optimal substrates of protein kinases. *Curr. Biol.* **4**:973–982.
81. **Srinivasan, J., M. Koszelak, M. Mendelow, Y. G. Kwon, and D. S. Lawrence.** 1995. The design of peptide-based substrates for the cdc2 protein kinase. *Biochem. J.* **309**:927–931.
82. **Sturman, L. S., and K. K. Takemoto.** 1972. Enhanced growth of a murine coronavirus in transformed mouse cells. *Infect. Immun.* **6**:501–507.
83. **Wege, H., S. Siddell, and V. ter Meulen.** 1982. The biology and pathogenesis of coronaviruses. *Curr. Top. Microbiol. Immunol.* **99**:165–200.
84. **Weinberg, R. A.** 1995. The retinoblastoma protein and cell cycle control. *Cell* **81**:323–330.
85. **Wiebusch, L., and C. Hagemeier.** 1999. Human cytomegalovirus 86-kilodalton IE2 protein blocks cell cycle progression in G<sub>1</sub>. *J. Virol.* **73**:9274–9283.
86. **Wurm, T., H. Chen, T. Hodgson, P. Britton, G. Brooks, and J. A. Hiscox.** 2001. Localization to the nucleolus is a common feature of coronavirus nucleoproteins, and the protein may disrupt host cell division. *J. Virol.* **75**:9345–9356.
87. **Yang, D. Q., and M. B. Kastan.** 2000. Participation of ATM in insulin signalling through phosphorylation of eIF-4E-binding protein 1. *Nat. Cell Biol.* **2**:893–898.
88. **Yarosh, D. B., P. D. Cruz, I. Dougherty, N. Bizios, J. Kibitel, K. Goodtsova, D. Both, S. Goldfarb, B. Green, and D. Brown.** 2000. FRAP DNA-dependent protein kinase mediates a late signal transduced from ultraviolet-induced DNA damage. *J. Investig. Dermatol.* **114**:1005–1010.
89. **Yu, H., B. Bauer, G. K. Lipke, R. L. Phillips, and G. Van Zant.** 1993. Apoptosis and hematopoiesis in murine fetal liver. *Blood* **81**:373–384.
90. **Zhang, J., R. J. Sanchez, S. Wang, C. Guarnaccia, A. Tossi, S. Zahariev, and S. Pongor.** 1994. Substrate specificity of CDC2 kinase from human HeLa cells as determined with synthetic peptides and molecular modeling. *Arch. Biochem. Biophys.* **315**:415–424.